Alexander L. Perryman[1]*
Jung-Hsin Lin[2]
J. Andrew McCammon[1,3]
[1] *Howard Hughes Medical Institute, Center for Theoretical Biological Physics, and Department of Pharmacology, University of California at San Diego, La Jolla, CA 92093-0365*

[2] *School of Pharmacy, National Taiwan University, Taipei, 100, Taiwan*

[3] *Department of Chemistry and Biochemistry, University of California at San Diego, La Jolla, CA 92093-0365*

Restrained Molecular Dynamics Simulations of HIV-1 Protease: The First Step in Validating a New Target for Drug Design

Received 5 December 2005; revised 21 February 2006; accepted 22 February 2006
Published online 28 February 2006 in Wiley InterScience (www.interscience.wiley.com). DOI 10.1002/bip.20497

Abstract: *To test the anticorrelated relationship that was recently displayed in conventional molecular dynamics (MD) simulations, several different restrained MD simulations on a wild type and on the V82F/I84V drug-resistant mutant of HIV-1 protease were performed. This anticorrelated relationship refers to the observation that compression of the peripheral ear-to-cheek region of HIV protease (i.e., the elbow of the flap to the fulcrum and the cantilever) occurred as the active site flaps were opening, and, conversely, expansion of that ear-to-cheek region occurred as both flaps were closing. An additional examination of this anticorrelated relationship was necessary to determine whether it can be harnessed in a useful manner. Consequently, six different MD experiments were performed that incorporated pairwise distance restraints in that ear-to-cheek region (i.e., the distance between the α-carbons of Gly40 and Gln61 was restrained to either 7.7 or 10.5 Å, in both monomers). Pushing the backbones of the ear and the cheek regions away from each other slightly did force the flaps that guard the active site to remain closed in both the wild type and the mutant systems—even though there were no ligands in the active sites. Thus, these restrained MD simulations provided evidence that the anticorrelated relationship can be exploited to affect the dynamic behavior of the flaps that guard the active site of HIV-1 protease. These simulations supported our*

Correspondence to: Alexander L. Perryman, at present address: Prof. Steve L. Mayo's Lab, HHMI/Caltech 114-96, 1200 E. California Blvd., Pasadena, CA 91125-9600; e-mail: aperryma@caltech.edu or aperryma@mccammon.ucsd.edu

Contract grant sponsor: Howard Hughes Medical Institute, W. M. Keck Foundation, NIH, NSF, NPACI/SDSC, NBCR, and UCSD's NSF Center for Theoretical Biological Physics (CTBP).

*Recent graduate of the Biomedical Sciences Ph.D. Program at UCSD.

Biopolymers, Vol. 82, 272–284 (2006)

© 2006 Wiley Periodicals, Inc.

WILEY InterScience® DISCOVER SOMETHING GREAT

hypothesis of the mechanism governing flap motion, and they are the first step towards validating that peripheral surface as a new target for drug design. © 2006 Wiley Periodicals, Inc. Biopolymers 82: 272–284, 2006

This article was originally published online as an accepted preprint. The "Published Online" date corresponds to the preprint version. You can request a copy of the preprint by emailing the Biopolymers editorial office at biopolymers@wiley.com

Keywords: *HIV-1 protease; V82F/I84V drug-resistant mutant; molecular dynamics, structure-based drug design; drug resistance; drug target validation; molecular modeling; relaxed complex method of flexible drug design; allosteric inhibitor; computational structural biology; theoretical biochemistry*

INTRODUCTION

According to the United Nations website, www.unaids.org, they estimate that in the year 2005 there were over 40 million people living with an HIV (human immunodeficiency virus) infection. Over three million people died from the AIDS epidemic, and approximately five million people became infected with HIV in 2005 alone. AIDS has already killed more humans than the bubonic plague.

HIV protease is one of three enzymes involved in that viral infection (the other two being HIV reverse transcriptase and HIV integrase). The first anti-AIDS drugs to appear were the reverse transcriptase inhibitors. The creation of HIV protease inhibitors led to the development of the Highly Active Anti-Retroviral Therapy regime (i.e., the HAART "cocktail"), which involves a combination of reverse transcriptase and HIV protease inhibitors. The use of those HAART cocktails significantly extended the life spans of patients infected with HIV. Because of the success of those HIV protease inhibitors (in combination with the reverse transcriptase inhibitors), a diagnosis of an HIV infection is no longer an immediate death sentence—patients on those HAART cocktails can now live productive lives for more than a decade. Unfortunately, in the past few years, drug-resistant strains of HIV have become more common and more deadly. When the strains of HIV from recently infected patients were examined, an alarming increase in drug resistance was discovered. In just a few years, the distribution of strains that were highly resistant to one drug increased from 3.4% (during the 1995–1998 period) to 12.4% (measured during the 1999–2000 period), and the frequency of HIV strains resistant to multiple different drugs simultaneously increased from 1.1 to 6.2%.[1] The fact that the entire pool of viral strains within the United States is shifting to become more and more drug resistant indicates a profound need to both understand the mechanisms of drug resistance and to develop truly novel approaches for treating HIV infections.

From the results of 22 nanosecond-long, conventional, all-atom, explicitly solvated molecular dynamics simulations of a wild type (1KZK.pdb)[2] and of the V82F/I84V drug-resistant mutant of HIV-1 protease, valine 82 mutated to phenylalanine and isoleucine 84 mutated to valine (1D4S.pdb),[3] a plausible reason to explain the drug-resistant properties of that double mutant was discovered.[4] Those molecular dynamics (MD) experiments indicated that the mechanism of drug resistance for that double mutant potentially involves a shift in its ensemble of conformations such that the mutant favors the semiopen structures more than the wild-type protease prefers them. The V82F/I84V mutant displayed a pattern of increased flap-opening behavior relative to the wild-type system (the mutant's flaps sampled much larger flap–catalytic Asp distances, and they experienced many more opening events). Because a large enthalpic cost is involved when an inhibitor forces the flaps of HIV-1 protease to close,[18] the drugs would have to pay a larger energetic penalty when closing the flaps of a mutant protease that displays a larger preference for the semiopen conformations. This could explain why all of the different HIV-1 protease inhibitors have worse affinity with this mutant.[4] In addition, an anti-correlated relationship observed in those studies suggested that the peripheral surface of HIV protease has the potential to be a new target for drugs that could allosterically regulate the opening/closing behavior of the flaps that control access to the active site.[4]

In one of the earliest MD simulations of HIV-1 protease—a 100-ps simulation performed using the GROMOS86 force field—the presence of similar correlated motions was observed, and the fact that this enzyme functions as a holistic entity was noted,[5,6] but the authors did not observe substantial flap displacements in that very short simulation, and no discussion was made regarding the exploitation of those corre-

lated motions for a pharmaceutical purpose. In addition, an anticorrelated relationship between the ear and the flap to which it is connected was present in the dynamic cross-correlation maps (DCCMs) from studies of HIV protease by the Karplus Group, but it was never discussed.[7] In a different simulation, when harmonic restraints were applied that pushed apart the α-carbons of residues 68–39, 168–139, 69–40, and 169–140 for a 0.35 ns MD run, the flaps then pushed the substrate down towards the catalytic aspartates.[8] In their subsequent round of experiments, they performed MD simulations that indicated the M46I compensatory mutant of HIV-1 protease displays differences in the flexibility of its flaps, relative to a wild-type system.[9] In direct contrast to our conclusions regarding the V82F/I84V drug-resistant mutant, they suggested that the M46I compensatory mutant stabilized the closed conformation and displayed less flexibility in its flaps, which could explain an increased catalytic rate for that mutant.[9] Because HIV protease utilizes a complex mechanism of action that involves numerous, large structural transitions, it does make sense that different mutations could affect binding and catalysis in different manners. The drug-resistant mutants must be able to both evade the binding of drugs (which are usually peptidomimetic) and simultaneously allow the efficient binding and cleavage of polypeptide substrates. Stabilizing the closed conformation with the M46I mutation could increase the rate of catalysis of its natural viral polypeptide substrate, and stabilizing the semiopen conformations with the V82F/I84V mutations would force drugs to pay a larger energetic penalty when binding. Thus, these hypotheses of the effects of different mutations are not contradictory or counterintuitive. Studying the combination of the compensatory mutant M46I with the drug-resistance mutations V82F/I84V would be interesting.

Although aspects of this anticorrelated relationship have been presented in the past by other groups, we were the first to suggest that the dynamic relationship indicates that the peripheral surface has the potential to be a binding site for allosteric inhibitors, and we are now the first to show that that relationship can indeed be exploited to affect flap motion in a pharmacologically useful manner. Those flaps must open before a substrate can access the active site, close completely before catalysis can occur, and again reopen to allow the products to leave and the next substrate to enter, before additional catalytic cycles can proceed. Thus, the ability to affect flap motion has significant implications with respect to inhibiting HIV-1 protease, which is one of the main targets for the treatment of AIDS.

To test this anticorrelated relationship, six different restrained MD simulations were performed on the wild type and on the V82F/I84V drug-resistant mutant of HIV-1 protease, using the exact same input files and the same AMBER7 molecular modeling platform[10] that were utilized in the aforementioned conventional MD studies.[4] This particular V82F/I84V double mutant of HIV-1 protease was selected because those two conservative mutations/monomer cause an 11-fold to a 2000-fold reduction in the binding affinity of all of the active-site HIV protease inhibitors that are currently used clinically.[11–13] Specifically, to test the exploitability of that anticorrelated relationship, six different 17 nanosecond-long, all-atom, explicitly solvated MD simulations were performed that incorporated harmonic, pairwise distance restraints in the peripheral ear-to-cheek region (see Figure 1 for a presentation of the topological nomenclature being used). That is, distance "Z," the distance between the α-carbons of Gly40 and Gln61,

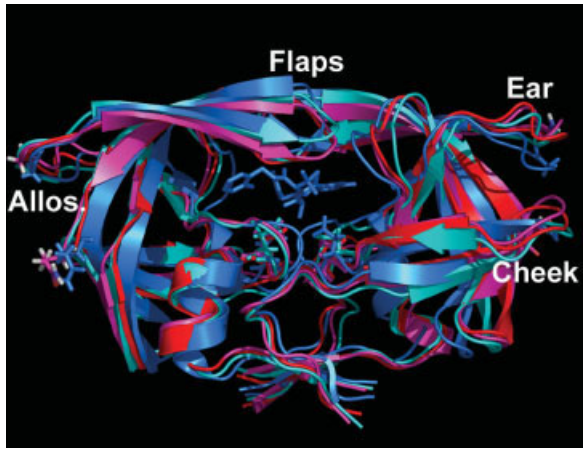

FIGURE 1 Comparing the wild-type crystal structure to snapshots from the MD runs with the flap-closing restraints: the crystal structure of the wild-type HIV-1 protease bound to the putative drug JE-2147 is shown in blue, and the ligand is depicted as the blue sticks in the center. The topological nomenclature that we proposed is labeled in white. "Allos." indicates the "allosteric groove," which refers to the ear-to-cheek interface region. Only the wild-type crystal structure contains a ligand—the other three structures have a closed conformation, because restraints were applied that slightly expanded that peripheral ear-to-cheek region, which prevented flap-opening behavior. In the red, magenta, and cyan structures, the distance between residues Gly40 and Qln61 (distance *Z*, shown by the pair of residues in stick mode on the sides) in each monomer was restrained to the value of 10.5 Å. As a reference, the closed crystal structure displays a value of 9.6 Å for that distance. The cyan cartoon represents the 16,000th picosecond snapshot from the wild-type MD run shown in red in Figure 3, and the red and magenta ribbons display the 15,710th and the 15,816th picosecond snapshots from the mutant MD run shown in red in Figure 5.

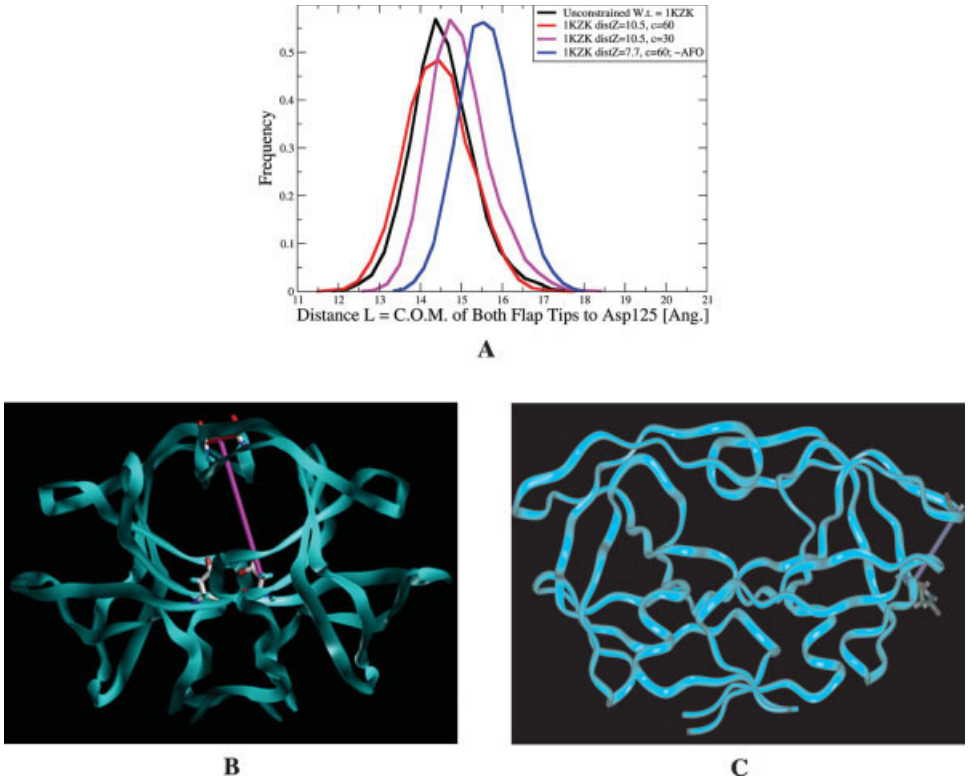

FIGURE 2 Histograms of the distance between the center of mass of the top of both flap tips to a catalytic Asp: the distance between the center of mass of Gly51 and Gly151 to the β-carbon of Asp125 (i.e., distance *L*, which is shown as the magenta stick on the ribbon diagram on the left) was measured in these three restrained wild-type MD experiments and compared to the histogram from 15 nanoseconds (the 3rd to the 17th nanoseconds) of our previous conventional wild-type MD run. All four simulations began with the exact same structure of the closed conformation of the apo wild-type protease (that is, the inhibitors were deleted from the active sites before beginning the MD runs). Distance *Z*, the distance that was restrained, is displayed as the purple stick on the ribbon diagram on the right. The black curve displays the histogram from the conventional, unrestrained wild-type MD simulation, which did not display significant flap-opening behavior. The red and magenta histograms represent the values from 15,000 snapshots from the MD simulations restrained to keep the flaps closed (i.e., to mimic the effects of an allosteric flap closer). Conversely, the blue histogram demonstrates the effects of an allosteric flap opener. Because the restraints utilized to generate the data shown by the blue histogram were chosen to mimic the effects of an allosteric flap opener, the symbol AFO is included for that line of the figure legend. For comparison, distance *L* had a value of 15.0 Å in the closed crystal structure of the complex of HIV-1 protease with an active-site inhibitor (1KZK.pdb)[2], and it had a value of 19.7 Å in the semiopen crystal structure of the apo HIV-1 protease (1HHP.pdb).[14]

was restrained to either 7.7 or 10.5 Angstroms in both monomers of each system; see Figures 1 and 2 for the location of those residues.

The values of the restraints were chosen to reflect gentle restraints and to cause minimal perturbations. The value of 7.7 Å was chosen, because that is the value of the mutant's peak in the histogram of distance *Z* in our previous publication. That is, clamping the peripheral distance *Z* to 7.7 Å should favor flap opening, since the conventional mutant MD trajectory that was the source of the data in that histogram displayed substantial flap-opening behavior. Similarly, the value of 10.5 Å was selected, because that is the value of the peak of the wild type's histogram of distance *Z* in the previous study. Restraining distance *Z* (in both monomers) to force it to remain at 10.5 Å should inhibit flap-opening behavior, because the conventional wild-type MD trajectory that was the source of the data in that histogram did not display significant flap-opening behavior. As a reference, distance *Z* had a value of 9.6 or 9.7 Å in the wild type and in the drug-resistant mutant's crystal structures,

respectively (both are inhibitor-bound, closed complexes). Because pushing the backbones of the ear and the cheek regions away from each other slightly (i.e., less than 1 Å) did force the flaps that guard the active site to remain closed (even though no substrate was present), this supported our previously published conclusions and provided evidence that facilitates the process of validating this peripheral surface as a potential new target for drug design.

These simulations began with the unbound form of the closed conformation of HIV protease. The 1KZK.pdb and the 1D4S.pdb crystal structures of the complexes of wild type or mutant HIV-1 protease (respectively) with an inhibitor were downloaded from the Protein Data Bank (PDB). The inhibitors were deleted and replaced with water before our calculations were initiated. We chose this protocol for our initial MD studies of the HIV-1 protease system[4] to generate ensembles of target conformations that were not biased by the presence of any particular inhibitor. In addition, we chose this protocol because we thought it should enable us to observe large flap displacements, and it did. As the apo protease thermodynamically favors the semiopen conformations, our far from equilibrium approach that utilized the unbound form of the closed conformation facilitated the large flap motions that we observed. This rationale is supported by a short MD simulation performed by the Karplus Group.[7] We chose to follow the exact same protocol in these restrained simulations, because we wanted to be able to make a direct comparison of the statistics from these simulations to those from our previously published simulations (calculations that took about a year to generate). In addition, many different groups have published simulations that involved the closed complex of HIV protease bound to an inhibitor or peptide substrate (simulations in which only minor structural changes were observed). We thought we would be able to learn more by following our novel approach than by mimicking previous simulations already performed by other groups, and we wanted to be able to make a fair comparison between our new results and our previous data (to help reduce the computational costs).

While these six restrained, all-atom, explicitly solvated, conventional MD simulations were being performed, an independent, coarse-grained simulation of the dynamics of wild-type HIV-1 protease was occurring simultaneously in which full opening of the flaps was observed many times.[15] The exact same anticorrelated relationship was observed in those coarse-grained simulations. When the peripheral ear-cheek regions were then restrained to force them to have the values they assume when the flaps are closed, then no flap opening was allowed. Thus, the restrained, coarse-grained simulations in that study also demonstrated that a hypothetical allosteric inhibitor could prevent flap-opening behavior,[15] which adds additional support to our conclusions.

MATERIALS AND METHODS

For a detailed description of the methods used in the MD simulations, see Ref. 4. The wild-type and the mutant simulations in that study began with the closed crystal structures of the complexes of those protease molecules with active-site inhibitors, the inhibitors were deleted and replaced with water molecules, and then the MD runs were initiated on the closed forms of the apo protease molecules. All crystal structures were downloaded from the PDB.[19] The first picosecond snapshots from the production phases of the conventional MD simulations described in our previous publication[4] were used as the input files for these restrained MD experiments. That is, the exact same files for the equilibrated snapshots used as the inputs for those conventional MD experiments in our previous study were used as the input files for these restrained trajectories. The only difference in these six new simulations was the application of two pairwise distance restraints to each homodimer (i.e., one restraint was applied to distance Z in the ear-to-cheek region of each monomer, see Figure 2). A force constant of either 30 or 60 kcal/mol/Å^2 was used to clamp distance Z (the distance from the α-carbon of Gly40 in the tip of the ear to the α-carbon of Gln61 in the β-sheet of the cheek region, and the corresponding distance in the other monomer), such that it remained at a constant value. Two of the restrained MD simulations had distance Z restrained to 7.7 Å, while the other four restrained MD simulations had distance Z clamped to 10.5 Å.

Each restrained MD experiment was performed for 17 ns, and statistics were calculated on the last 15 ns of each trajectory and compared to the statistics from the 2000th to the 17,000th picosecond snapshots from the conventional MD simulations described in our previous publication. Thus, these restraints tested the anticorrelated relationship discovered in the experiments discussed in our previous study[4] to examine whether our hypothesis of the mechanism of flap motion was correct and whether it could be harnessed in a useful manner. Similarly, these restraints also allowed for the simultaneous investigation of the effects of imaginary allosteric inhibitors binding to that peripheral ear-to-cheek surface (i.e., these restrained MD simulations produced support for the process of validating that peripheral surface as a new target site for drug design).

For a detailed description of the relaxed complex method of drug design, see Refs. 16 and 17. To prepare for relaxed complex studies against HIV protease, a plethora of AutoDock3.0.5 calculations[20] with different run parameters and preparation protocols were performed to optimize the speed and the accuracy of the control experiments. The control case involved calculating the structure of the complex

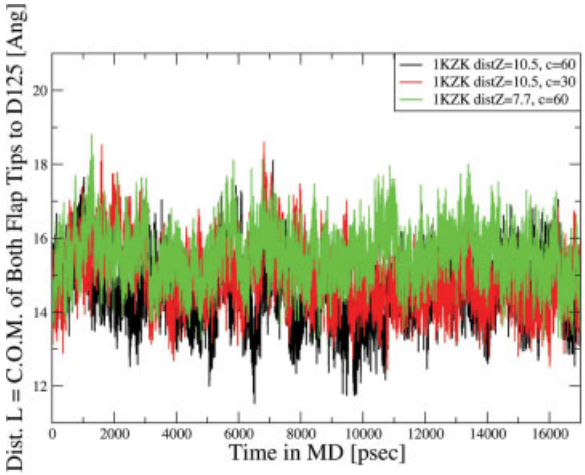

FIGURE 3 The above graph displays the 17 nanosecond-long trajectories of the data that are plotted as histograms in Figure 2. The black and red trajectories correspond to the wild-type simulations that were restrained to keep their flaps closed (i.e., to the red and magenta histograms in Figure 2, respectively), while the green trajectory represents the wild-type simulation that involved restraints that attempted to force the flaps to open (i.e., it corresponds to the blue histogram in Figure 2). As a reference, distance *L* represents the distance from the β-carbon of catalytic Asp125 to the center of mass of the top of both tips of the flaps, while distance *Z* measures the distance between the α-carbons of Gly40 and Gln61 (in the ear and the cheek, respectively).

of wild-type HIV-1 protease with the second-generation inhibitor JE-2147 (also known as the putative drug SM-319777 or KNI-764), and the accuracy of the control experiments was judged by their ability to reproduce the 1KZK.pdb crystal structure of the complex.[2] Although a few of the initial sets of parameters did accurately reproduce this crystal structure of the complex, subsequent control experiments were done to enrich the percentage of runs that produced the correct result and to decrease the amount of CPU time required per job.

The all-atom runs took much more than twice as long and were not nearly as accurate, while the united atom runs were consistently correct and finished much more quickly. The best preparation protocol and set of AutoDock3.0.5[20]-run parameters for docking to the crystal structure of this particular system (which involved a ligand with 11 active torsions that is docked into a tunnel composed of the active site and the flaps that enclose it) were as follows: the united atom representation for both protein and ligand (i.e., the nonpolar hydrogen atoms were merged onto their respective heavy atoms, which produced the set of atom types composed of CANOSH) was used, random values for the initial dihedral angles of the ligand were generated, a focused docking approach was used (the center of the grid was located at one of the oxygen atoms of the carboxylate group (OD1) of the catalytic residue Asp 25, and the grid size was $70 \times 70 \times 70$ points, with 1 point corresponding to 0.375 Å), only 1000 generations were used (instead of the default value of 27,000), a population size of 150 was selected (rather than the default of 50), and an ls_search_frequency of 0.07 was used (as opposed to the default of 0.06). But many different sets of run parameters did reproduce the correct binding mode—the previous parameter set just describes the most accurate job settings when docking against that crystal structure. However, for relaxed complex purposes the best set of run parameters for docking to every 10th picosecond snapshot from those MD trajectories (as judged by both their speed and reproducibility against an

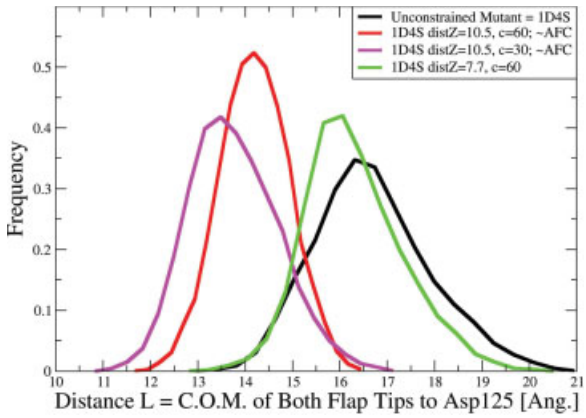

FIGURE 4 Histograms of the distance between the center of mass of the top of both flap tips to a catalytic Asp in the mutant systems: the distance between the center of mass of Gly51 and Gly151 to the β-carbon of Asp125 (i.e., distance *L*) was measured in these three restrained MD simulations of the V82F/I84V drug-resistant mutant of HIV-1 protease and compared to the histogram from 15 ns of our previous conventional mutant MD run. All four simulations began with the exact same structure of the closed conformation of the apo mutant protease (that is, the inhibitors were deleted from the active sites before beginning the MD runs). The black curve displays the histogram from the conventional, unrestrained mutant MD simulation, which displayed substantial flap-opening behavior. The red and magenta histograms depict the values from the mutant MD simulations that were restrained to keep the flaps closed (i.e., to mimic the effects of an allosteric flap closer) by expanding that peripheral ear to cheek distance to 10.5 Å with a force constant of either 60 or 30 kcal/mol/Å^2, respectively. Conversely, the green histogram displays the effects of an imaginary allosteric flap opener (i.e., by forcing distance *Z*, the distance from the α-carbons of Gly40 and Gln61, to remain at 7.7 Å, flap-opening behavior was allowed). Because the restraints utilized to generate the data shown by the red and magenta histograms were chosen to mimic the effects of an allosteric flap closer, the symbol AFC is included for those lines of the figure legend. As a reference, a value of 19.7 Å for distance *L* can be considered as one type of relative signature of the semi-pen state, as defined by a semiopen crystal structure of the apo HIV-1 protease (1HHP.pdb).[14]

ensemble of conformations) differed from the above set by using a population size of only 50 and by using just 750 generations. When each snapshot was targeted in one relaxed complex experiment, 10 separate docking attempts were performed, and the best of those 10 attempts was selected. Each docking attempt involved hundreds of generations, and each generation involved hundreds of thousands of energy evaluations. The exact same preparation protocol and run parameters from the relaxed complex experiments on the wild-type system were utilized in the studies of the mutant system. The open source program PyMOL[22] was used to generate some of the molecular graphics utilized in these figures.

RESULTS

Because distance *Z* (the distance between the α-carbons of Gly40 and Gln61, see Figures 1 and 2) displayed the anticorrelated relationship with distance *L* (the distance from the β-carbon of the catalytic Asp125 to the center of mass of the top of both tips of the flaps, see Figure 2), and because one goal was to examine whether an imaginary allosteric inhibitor that binds to the peripheral ear-to-cheek interface actually has the ability to affect the opening and/or closing behavior of both active site flaps, the analyses of these restrained simulations focused on the effects that the restraints had upon the dynamics of distance *L*.

Although the effects of those restraints were somewhat minor for the wild-type histograms displayed in Figure 2 and for the trajectories shown in Figure 3, the restraints that were applied were fairly gentle (i.e., the allosteric flap-opening restraint involved a change of slightly less than 1 Å from the starting crystal structure, while the allosteric flap-closing restraint was a shift of only 2 Å), and the unrestrained wild-type MD simulation to which they were being compared did not display significant flap-opening behavior. Although there are many possible ways to define the closed and semiopen states, the relative definitions used herein were based upon the flap–Asp distances displayed in the 1HHP.pdb crystal structure of a semiopen conformation of HIV-1 protease.[14] The initial, unrestrained wild-type protease remained closed during the first 17 ns of that simulation: one wild-type flap briefly flickered into a semiopen state, but the other flap was always closed (see Figures 2 and 3). However, those restraints did still serve their purpose. When distance *Z* was clamped to 10.5 Å in these restrained wild-type MD simulations, the flaps never opened (i.e., their histograms overlapped substantially with the histogram from the unrestrained wild-type MD run from our previously published results). Conversely, when distance *Z* was restrained to 7.7 Å, that restrained wild-type system did experience more flap-opening behavior than the other three wild-type MD simulations displayed (i.e., the histogram of the MD run with the allosteric flap-opening restraint was shifted towards more open flap values by more than 1 Å). In general, the green trajectory produced by the allosteric flap-opening restraint was above the black and red trajectories produced by the allosteric flap-closing restraints. This observation does coincide with the trends observed in the histograms. Thus, the wild-type MD run with the flap-opening restraints did sample larger values for distance L—its flaps opened more fully and more often than they did in the other three MD simulations of the wild-type system.

The effects of those restraints were much more pronounced in the mutant system; however, the conventional mutant MD simulation to which they were being compared actually sampled substantial flap-opening behavior, which was most likely due to the indirect effects of those two drug-resistance mutations.[4] In both a qualitative examination of the trajectories of the 17 nanosecond-long restrained mutant MD simulations and in the histograms of the statistics of the sampling behavior that occurred during the last 15 ns of each system (from the 2000th to the 17,000th-ps snapshots), the effects of those restraints were quite clear. When the V82F/I84V mutant system had that peripheral distance *Z* held constant at 10.5 Å, then flap-opening behavior was suppressed severely (see Figures 1 and 4–6).

The two mutant MD simulations with the flap-closing restraints even demonstrated sampling behavior similar to the unrestrained wild-type simulation (those three histograms all have similar ranges and have peaks less than 14.5 Å), which highlights the extent to which flap-opening behavior was inhibited in the mutant system by the imaginary allosteric flap closer. Thus, allosteric flap-closing inhibitors have the potential to rescue the efficacy of the current active site inhibitors by restoring their effectiveness against the drug-resistant mutants, due to their ability to restore near-wild type flap behavior to this mutant.

Similarly, there was substantial overlap between the histogram of the unrestrained mutant simulation (which displayed significant flap-opening behavior) and the histogram from the mutant simulation that had the flap-opening restraints. Thus, when that peripheral distance was forced to remain at 7.7 Å in that restrained mutant MD simulation, then substantial flap-opening behavior was allowed to occur (see Figures 4–6). Although the allosteric flap-opening restraint did allow flap-opening behavior, it did not enhance it.

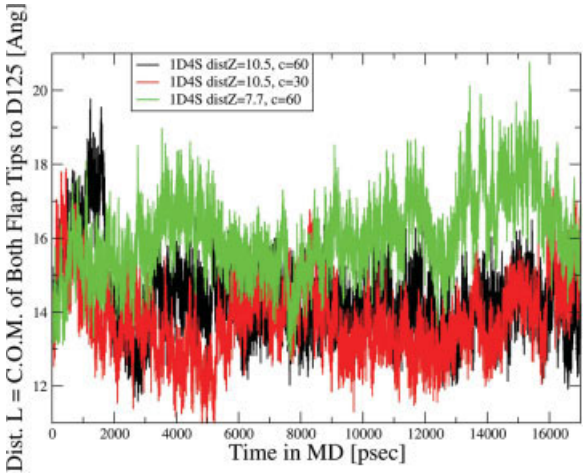

FIGURE 5 The above graph displays the 17 nanosecond-long trajectories of the data that are plotted as histograms in Figure 4. The black and red trajectories correspond to the simulations of the drug-resistant V82F/I84V mutant restrained to keep their flaps closed (i.e., to the red and magenta histograms from Figure 4, respectively), while the green trajectory represents the mutant simulation restrained in a manner that attempted to force the flaps to open (i.e., it corresponds to the green histogram in Figure 4). The allosteric flap closing restraints did suppress flap-opening behavior in both simulations, and the allosteric flap opening restraints did allow flap-opening behavior.

Though it has been shown that these restraints on the peripheral ear-to-cheek regions did affect the dynamic motion of the flaps in both the wild-type and the mutant systems, the general structure of HIV-1 protease was well maintained in these restrained simulations (see Figures 1 and 6). The snapshots from the restrained MD simulations do superimpose well on the structure of the wild-type crystal structure. Besides affecting the sampling behavior of the flaps, the only other significant effect of those restraints was a slight disruption in the secondary structure in the region adjacent to the restrained residues. This disruption is highlighted by the differences between the cartoons of the restrained conformations and the ribbon of the wild-type crystal structure in Figure 1. In addition, these restraints did not perturb the dynamics of the active sites' structures in a deleterious manner, as judged by indirect evidence provided by docking the putative drug JE-2147 (also known as SM-319777, or KNI-764) to every 10th picosecond snapshot from these MD simulations. That is, when the relaxed complex method of drug design[16,17] was applied to the conformations harvested from these conventional and restrained MD simulations, the profiles of the free energy of binding of that second-generation inhibitor demonstrated that these restrained MD simulations produced conformations to which that active-site inhibitor binds extremely well (as compared to the conventional, unrestrained MD simulations).

An appropriate preparation protocol and set of AutoDock run parameters for the docking phase of the relaxed complex method was discerned during control studies that involved reproducing the crystallographic binding mode of the putative drug JE-2147 with the wild-type HIV-1 protease (1KZK.pdb)[2] (see Figure 7—and Figure 1). That approach was then utilized in relaxed complex experiments against the two ensembles of conformations from the unrestrained MD simulations of the wild-type and of the mutant protease and also against the four ensembles of conformations from the MD simulations generated with the flap-closing restraints. As can be seen in Figure 8,

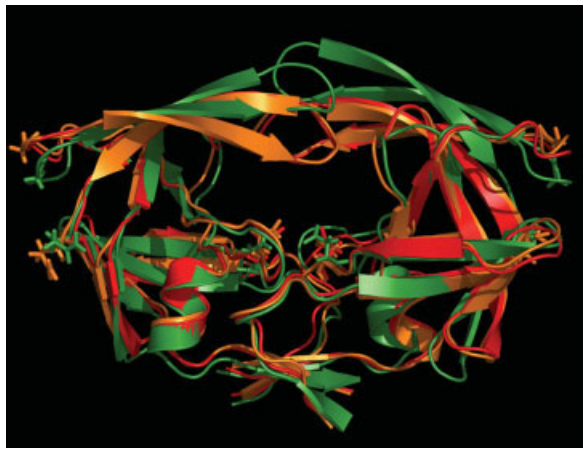

FIGURE 6 Effects of imaginary allosteric inhibitors on flap motion: the distances between the peripheral residues Gly40 to Gln61 and Gly140 to Gln161, shown as the pairs of residues represented as sticks on the sides, were restrained to either 7.7 or 10.5 Å during these MD runs. The green representation of the 15,355th ps snapshot from the mutant MD trajectory shown in green in Figure 5 demonstrates that slightly compressing the peripheral ear-to-cheek region does allow opening of the flaps to occur. Conversely, although no ligands were present in any of these simulations, when the peripheral surfaces were restrained to remain at an expanded value, then the flaps could not open, as shown by the red and the orange ribbons from the 15,710th and the 15,816th ps snapshots from the mutant MD trajectory shown in red in Figure 5. As a reference, the flap-to-Asp distances (i.e., the values of distance *L*) were as follows: 20.74 Å for the conformation shown in green, 12.33 Å for the structure in red, 12.23 Å for the snapshot displayed in orange (or in magenta in Figure 1), 15.0 Å for the closed wild-type crystal structure (1KZK.pdb), and 19.7 Å in the semiopen crystal structure (1HHP.pdb). To enable a comparison with Figure 1, the wild type's cyan snapshot had a value of 13.06 Å for distance *L* in that image.

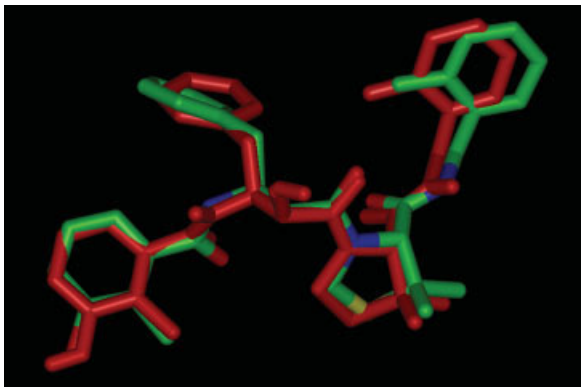

FIGURE 7 Accuracy of the control experiments when applying the relaxed complex method to the wild-type HIV-1 protease system: the above image compares the binding modes of the putative drug JE-2147 from the crystal structure of the complex,[2] colored by atom type to that from the AutoDock3.0.5 experiments, colored red. The enzymatic target, HIV-1 protease, is not displayed, but the ligand was docked in the proper location and orientation. The preparation protocol and optimized run parameters used in the docking studies did accurately reproduce the crystallographic binding mode of this highly flexible drug.

when that approach was repeated in three independent relaxed complex experiments against the unrestrained wild-type MD simulation's conformations, very robust results were obtained. That is, those three independent relaxed complex experiments produced trajectories of the binding free energies of that drug vs. the snapshot that was targeted that were very similar, which indicated the reproducibility of this method. This approach produced similarly robust results when it was used in relaxed complex experiments against the V82F/I84V mutant system (data not shown).

The binding free energy profiles produced by the relaxed complex experiments on the ensembles of conformations from the wild-type MD runs that used the flap-closing restraints were the same as the profile produced by targeting the ensemble of conformations harvested from the unrestrained wild-type MD simulation (see Figure 9). From Figure 2 it is apparent that the wild-type MD simulations with the flap-closing restraints displayed flap behavior similar to the unrestrained wild-type MD run (which did not display much flap-opening behavior at all). Similarly, when every 10th picosecond snapshot from the first 10 ns of those two restrained MD runs on the wild-type system was targeted in relaxed complex experiments, it produced profiles of the free energy of binding that superimposed on the energetic profile produced by targeting conformations from the unrestrained wild-type simulation. If those flap-closing restraints had perturbed the dynamics of the active site in a deleterious manner, then those restrained MD runs would have produced relaxed complex energy profiles that demonstrated worse binding affinities than the profile produced from targeting the unrestrained MD run's conformations. Thus, an allosteric flap-closing inhibitor should not impede the effectiveness of an active-site inhibitor against the wild-type HIV-1 protease.

The relaxed complex experiments against the V82F/I84V mutant of HIV-1 protease provided evidence supporting the notion that the peripheral surface has the potential to be a new target for drug design. The mutant MD simulations performed with the application of the flap-closing restraints displayed much less flap-opening behavior than the unrestrained mutant MD run (see Figure 4). Similarly, those restrained mutant MD runs produced conformations that displayed much better binding affinities than the conformations harvested from the conventional mutant MD run produced in the relaxed complex experiments (see Figure 10). Because the restrained MD simulations of the mutant protease

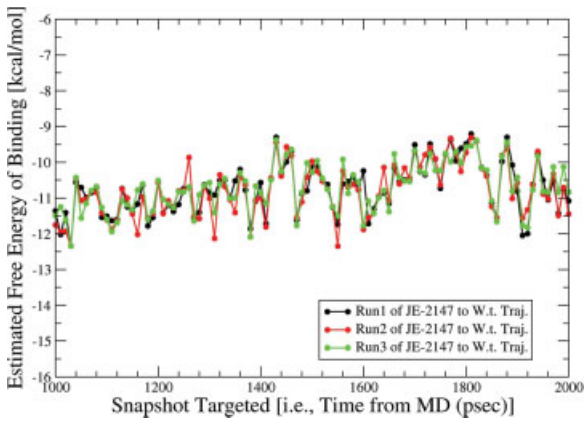

FIGURE 8 The relaxed complex method did produce robust results: the optimized run parameters that were used in the control study shown in Figure 7 did produce robust, reproducible results when utilized in three independent relaxed complex experiments. Each relaxed complex experiment involved docking the putative drug JE-2147 in a fully flexible manner to every 10th picosecond snapshot from our previously published MD simulations. When the relaxed complex experiment was repeated, a very similar trajectory of binding free energies was obtained in these three independent experiments, which demonstrates the robustness of this method. The filled circles on each trajectory indicate the particular snapshots that were targeted in those docking calculations. The second nanosecond interval from the wild-type MD simulation is shown, but the results were equally robust when targeting the entire 22 nanosecond trajectories from both the wild-type and the mutant MD simulations.

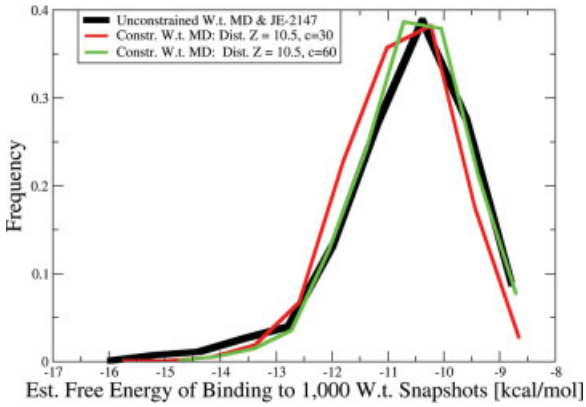

FIGURE 9 Comparing the relaxed complex results from the conventional wild-type MD simulation to the two restrained wild-type MD simulations: The exact same preparation protocol and run parameters were used in relaxed complex experiments involving these three different MD simulations of the wild-type HIV-1 protease. When the conventional, unrestrained wild-type MD simulation's snapshots were targeted in relaxed complex experiments, it produced a free energy of binding profile that is depicted by the black histogram. Similarly, the two wild-type MD simulations that utilized allosteric flap-closing restraints were targeted in relaxed complex experiments that produced the histograms shown in red and green. One thousand wild-type snapshots were targeted from each of the three simulations (i.e., every 10th picosecond snapshot from the first 10 nanoseconds of each simulation was harvested and utilized in the docking studies). If the flap-closing restraints had perturbed the dynamics of the active site in a deleterious manner, then the energetic profiles from the two restrained simulations would not display such a substantial overlap with the profile from the unrestrained simulation.

generated ensembles of conformations that had better affinity with this second-generation inhibitor than the unrestrained mutant ensemble of conformations demonstrated, this indicated that these flap-closing restraints could not have had a significant deleterious effect on the dynamics of the mutant's active site. Indeed, that those restrained mutant MD runs produced relaxed complex binding free energy profiles that were shifted towards better binding affinities indicates that the anticorrelated relationship can be exploited in a pharmacologically useful manner. Because these results indicate that an allosteric flap-closing inhibitor should be able to improve the effectiveness of an active-site inhibitor against that drug-resistant mutant of HIV-1 protease, these data are the first step in validating the peripheral surface of HIV protease as a new target for drug design. This potential new target, the "allosteric groove," is displayed in detail in Figure 11–13.

DISCUSSION

Because the restraints applied to the peripheral ear to cheek distance Z (from the α-carbon of Gly40 to the α-carbon of Gln61, see Figures 1, 2, and 6) had the predicted consequences, this provided support to the hypothesis that the anticorrelated relationship that we previously discussed does actually contribute to the mechanism that governs flap motion for HIV-1 protease. When gentle flap-closing restraints were applied to either the wild-type or to the V82F/I84V mutant systems (by forcing a slightly less than 1 Å expansion of that peripheral ear-to-cheek distance) in those 17 nanosecond-long MD simulations, flap-opening

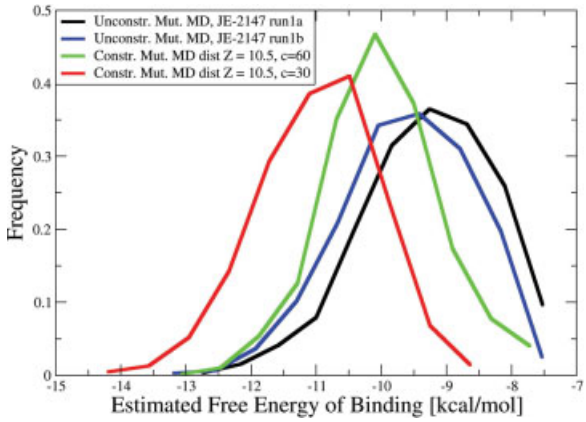

FIGURE 10 Comparing the relaxed complex results from the conventional V82F/I84V mutant MD simulation to two restrained mutant MD simulations: When the conventional, unrestrained mutant MD simulation's snapshots were targeted in two independent relaxed complex experiments, the free energy of binding profiles that are represented by the black and blue histograms were produced. Similarly, the two mutant MD simulations that utilized allosteric flap-closing restraints were targeted in relaxed complex experiments that produced the histograms shown in red and green. One thousand mutant snapshots were targeted from each of the three simulations (i.e., every 10th picosecond snapshot from the first 10 ns of each simulation was harvested and targeted in the docking studies). The unrestrained mutant MD simulation that was targeted displayed substantial flap-opening behavior (see Figure 4). The flap-closing restraints restored near wild-type flap behavior to the mutant system (i.e., they prevented the flaps from opening). Similarly, those flap-closing restraints produced conformations of the mutant protease that displayed much more favorable binding free energy profiles than the snapshots harvested from the unrestrained mutant MD simulation generated. Thus, by applying those restraints that slightly expanded the peripheral surface of HIV-1 protease, the binding affinity of an active site inhibitor with this drug-resistant mutant was improved (within our computational model).

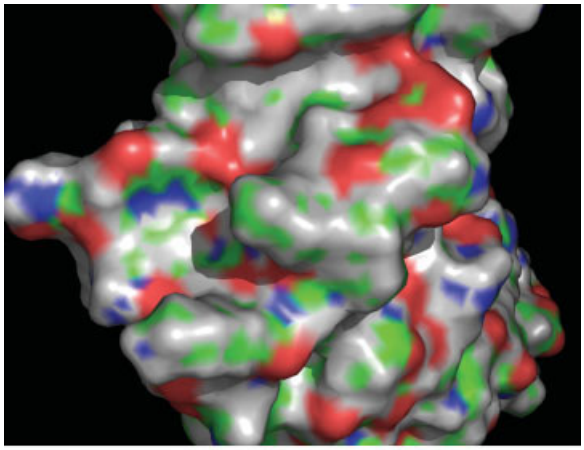

A

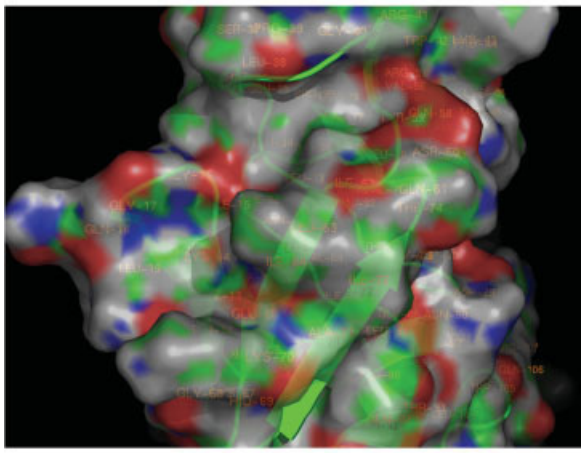

B

FIGURE 11 Solvent-accessible surface area of the allosteric groove from a closed mutant snapshot: the surface of the 15,710th picosecond snapshot from the mutant MD simulation performed with the allosteric flap-closing restraints (with a constant = 30 kcal/mol/Å^2, see Figures 1, 4, and 5) is shown, colored by atom type. The first image shows an opaque rendition of the solvent-accessible surface area (SASA), while the second image contains a semitransparent SASA so that the labels on the residues can be seen. This allosteric cleft has a suitable shape and many potential hydrophobic and polar interactions that could be complemented by an allosteric flap-closing inhibitor.

behavior was suppressed, even though there were no ligands in the active sites (see Figure 1). Similarly, the application of flap-opening restraints (by forcing a 2 Å compression of that peripheral ear-to-cheek distance) did allow the flaps to display opening behavior (see Figure 6). In addition, the mutant simulation with the flap-opening restraints did display more flap-opening behavior than the wild-type simulation with the flap-opening restraints demonstrated, which provided further support for our hypothesis of the mechanism of drug resistance for this V82F/I84V mutant.[4]

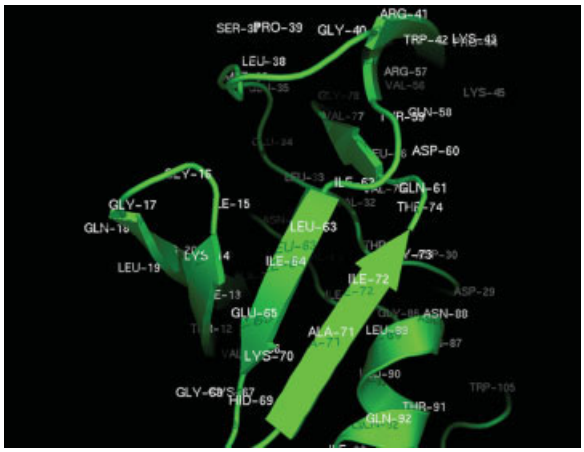

FIGURE 12 Labeled cartoon of the allosteric groove from a closed mutant snapshot: this image shows the exact same snapshot and the same view shown in Figure 11. For this representation of the 15,710th picosecond snapshot from the mutant MD simulation performed with the allosteric flap-closing restraints, only the backbone is shown, and all of the residues are labeled in white (at the positions of the α-carbons).

These restrained MD simulations not only provided support for our hypothesis of the mechanism that governs flap motion, the fact that this mechanism can be exploited in a pharmacologically useful manner also supports the notion that the peripheral ear-to-cheek interface (i.e., the "allosteric groove") does have the potential to be a new target for drug design. Due to the fact that the natural, viral polypeptide substrate of HIV-1 protease cannot access the active site until the flaps have opened, the fact that catalysis cannot occur until the flaps have closed completely, and the fact that the flaps must again reopen before the products can leave and allow a new catalytic cycle to proceed, an ability to control the opening/closing behavior of the flaps is by definition pharmacologically useful. In addition, because the flap-closing restraints did improve the binding affinity of the active-site inhibitor JE-2147 to those ensembles of the mutant's conformations, this clearly demonstrated the potential utility of an imaginary allosteric flap-closing inhibitor.

Because the effects of the flap-opening restraints were not as significant as those caused by the flap-closing restraints, this suggests that the drug design community should probably focus more on designing/discovering allosteric flap closers than on allosteric flap openers. Fortunately, the allosteric flap closers actually have the potential for synergism with the currently prescribed active-site protease inhibitors, due to their potential ability to help pay the large

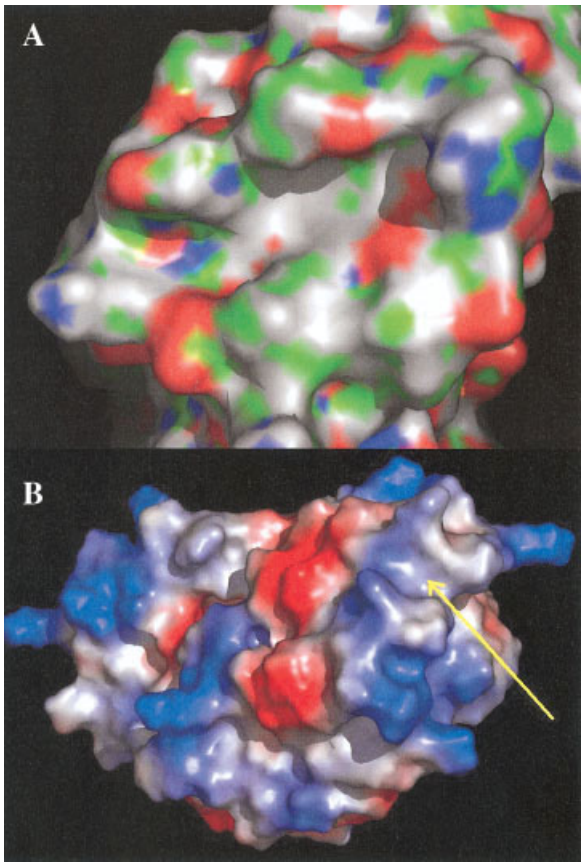

FIGURE 13 Solvent-accessible surface area of the allosteric groove from a semiopen mutant snapshot and from the wild-type crystal structure: the surface of the 15,355th picosecond snapshot from the mutant MD simulation performed with the allosteric flap-opening restraints (see Figures 4–6) is shown above, colored by atom type. The second image highlights the location of the allosteric groove (with an arrow) by showing the solvent-accessible surface area of the closed wild-type crystal structure, colored by its electrostatic potential (as calculated by APBS[21]). The allosteric groove in this semiopen mutant snapshot has a different shape than the cleft displays in the closed mutant snapshot and in the closed wild-type crystal structure, especially in the regions around Arg41 and Glu65 (see Figure 11).

enthalpic cost involved in closing the active site's flaps.[16] Indeed, when the flap-closing restraints were applied to the mutant MD simulations, the conformations they generated had significantly better binding affinities with a second-generation active-site inhibitor than the conformations from the unrestrained mutant MD run displayed (see Figure 10). In addition, the allosteric flap closers should be easier to develop on an intuitive level (i.e., it should be much less difficult to discover or design something that will bind to and expand that peripheral interface than to find something that would be able to compress it). Because the flap-closing restraints made the two restrained mutant systems behave in a near wild-type manner (with respect to motion of the flaps), which had a substantial effect on the binding affinity of the known inhibitor in our relaxed complex studies, this supports our previous conclusion that allosteric flap closers might be able to rescue the efficacy of the current protease drugs by synergistically improving their binding affinities against the mutants of HIV protease that currently impede drug treatment.[4]

No discussion was made concerning the physical properties of the putative allosteric inhibitors, because we do not yet have any data regarding actual allosteric inhibitors. The goal of this project was to use the application of a force to examine the biomechanical relationships that are present in the viral nanomachine that is HIV-1 protease. If these restrained MD simulations had not displayed the predicted consequences, then pursuing the design/discovery of those allosteric inhibitors would be quite a gamble. However, these restrained MD simulations did produce the predicted results, which is why these data are the first step towards validating that peripheral surface as a new target for drug design.

The comparison of these restrained MD simulations to our previous conventional MD simulations provided evidence regarding the mechanism that controls the behavior of the flaps that guard the active site of this important drug target. These restrained MD simulations showed that the anticorrelated relationship that likely controls closing of the active-site flaps can be exploited in a potentially useful manner: by causing a slight shift in the sampling properties of that peripheral ear-to-cheek distance, the ability of the active site's flaps to open can be suppressed. If the flaps of HIV protease cannot open properly, then its natural polypeptide substrates cannot enter that viral enzyme's active site, which means that catalysis cannot occur. If a peripheral inhibitor helps force the flaps to close, then that allosteric inhibitor would help pay the energetic cost that the active-site inhibitors currently have to pay by themselves (i.e., an allosteric flap-closing inhibitor should improve the effectiveness of the active-site inhibitors that are currently given to patients). Thus, these restrained MD simulations supported our hypothesis of the mechanism controlling flap motion, and they also simultaneously provided the first line of evidence that helps validate that peripheral ear-to-cheek interface as a potential new target for drug design.

We thank Dr. Robert Konecny for his computational assistance with the CTBP cluster. We thank Prof. Betsy Komives, Dean Palmer Taylor, Prof. Phil Bourne, Prof.

Susan Taylor, and Prof. Senyon Choe for their discussions, time, and advice. We also thank Dr. Donald Hamelberg, John Mongan, Jessica Swanson, and Dr. Jen Bui for their useful discussions. We thank the Howard Hughes Medical Institute and the W. M. Keck Foundation for their continued and generous financial support. We thank Accelrys, Inc., for their gift of InsightII. Additional support has been provided, in part, by grants to JAM from NIH, NSF, NPACI/SDSC, NBCR, and UCSD's NSF Center for Theoretical Biological Physics (CTBP). We thank the CTBP for dedicating several processors to this project. ALP was an HHMI Pre-doctoral Fellow, an affiliate of the Molecular Biophysics Training Grant, an affiliate of the CTBP, and a member of the Biomedical Sciences Graduate Program at UCSD. ALP thanks Prof. Steve Mayo and the Amgen Postdoctoral Fellowship program from the Division of Biology at Caltech for their current support.

REFERENCES

1. Little, S. J.; Holte, S.,; Routy, J. P.; Daar, E. S.; Markowitz, M.; Collier, A. C.; Koup, R. A.; Mellors, J. W.; Connick, E.; Conway, B.; Kilby, M.; Wang, L.; Whitcomb, J. M.; Hellmann, N. S.; Richman, D. D. N Engl J Med 2002, 347(6), 385–394.
2. Reiling, K. K.; Endres, N. F.; Dauber, D. S.; Craik, C. S.; Stroud, R. M. Biochemistry 2002, 41(14), 4582–4594.
3. Thaisrivongs, S.; Skulnick, H. I.; Turner, S. R.; Strohback, J. W.; Tommasi, R. A.; Johnson, P. D.; Aristoff, P. A.; Judge, T. M.; Gammill, R. B.; Morris, J. K.; Romines, K. R.; Chrusciel, R. A.; Hinshaw, R. R.; Chong, K. T.; Tarpley, W. G.; Poppe, S. M.; Slade, D. E.; Lynn, J. C.; Horng, M. M.; Tomich, P. K.; Seest, E. P.; Dolak, L. A.; Howe, W. J.; Howard, G. M.; Schwende, F. J.; Toth, L. N.; Padbury, G. E.; Wilson, G. J.; Shiou, L.; Zipp, G. L.; Wilkinson, K. F.; Rush, B. D.; Ruwart, M. J.; Koeplinger, K. A.; Zhao, Z.; Cole, S.; Zaya, R. M.; Kakuk, T. J.; Janakiraman, M. N.; Watenpaugh, K. D. J Med Chem 1996, 39(22), 4349–4353.
4. Perryman, A. L.; Lin, J.-H.; McCammon, J. A. Protein Sci 2004, 13(4), 1108–1123.
5. Harte, W. E.; Swaminathan, S.; Beveridge, D. L. Proteins Struct Funct Genet 1992, 13, 175–194.
6. Harte, W. E.; Swaminathan, S.; Mansuri, M. M.; Martin, J. C.; Rosenberg, I. E.; Beveridge, D. L. Proc Natl Acad Sci 1990, 87, 8864–8868.
7. Zoete, V.; Michielin, O.; Karplus, M. J Mol Biol 2002, 315(1), 21–52.
8. Piana, S.; Carloni, P.; Parrinello, M. J Mol Biol 2002, 319(2), 567–583.
9. Piana, S.; Carloni, P.; Rothlisberger, U. Protein Sci 2002, 11, 2393–2402.
10. Case, D. A.; Pearlman, D. A.; Caldwell, J. W.; Cheatham, T. E., III; Wang, J.; Ross, W. S.; Simmerling, C. L.; Darden, T. A.; Merz, K. M.; Stanton, R. V.; Cheng, A. L.; Vincent, J. J.; Crowley, M.; Tsui, V.; Gohlke, H., Radmer, R. J.; Duan, Y.; Pitera, J.; Massova, I.; Seibel, G. L.; Singh, U. C.; Weiner, P. K.; Kollman, P. A. AMBER 7, University of California, San Francisco, 2002.
11. Ohtaka, H.; Velazquez-Campoy, A.; Xie, D.; Freire, E. Protein Sci 2002, 11, 1908–1916.
12. Klabe, R. M.; Bacheler, L. T.; Ala, P. J.; Erickson-Viitanen, S.; Meek, J. L. Biochemistry 1998, 37(24), 8735–8742.
13. Ala, P. J.; Huston, E. E.; Klabe, R. M.; McCabe, D. D.; Duke, J. L.; Rizzo, C. J.; Korant, B. D.; DeLoskey, R. J.; Lam, P. Y. S.; Hodge, C. N.; Chang, C.-H. Biochemistry 1997, 36(7), 1573–1580.
14. Spinelli, S.; Liu, Q. Z.; Alzari, P. M.; Hirel, P. H.; Poljak, R. J. Biochemie 1991, 73(11), 1391–1396.
15. Tozzini, V.; McCammon, J. A. Chem Phys Lett 2005, 413, 123–128.
16. Lin, J.-H.; Perryman, A. L.; Schames, J. R.; McCammon, J. A. J Am Chem Soc 2002, 124(20), 5632–5633.
17. Lin, J.-H.; Perryman, A. L.; Schames, J. R.; McCammon, J. A. Biopolymers 2003, 68(1), 47–62.
18. Luque, I.; Todd, M. J.; Gomez, J.; Semo, N.; Freire, E. Biochemistry 1998, 37(17), 5791–5797.
19. Berman, H. M.; Westbrook, J.; Feng, Z.; Gilliland, G.; Bhat, T. N.; Weissig, H.; Shindyalov, I. N.; Bourne, P. E. Nucleic Acids Res 2000, 28, 235–242.
20. Morris, G. M.; Goodsell, D. S.; Halliday, R. S.; Huey, R.; Hart, W. E.; Belew, R K.; Olsen, A. J. J Comput Chem 1998, 19(14), 1639–1662.
21. Baker, N. A.; Sept, D.; Joseph, S.; Holst, M. J.; McCammon, J. A. Proc Natl Acad Sci USA 2001, 98, 10037–10041.
22. DeLano, W. L. The PyMOL Molecular Graphics System, DeLano Scientific, San Carlos, CA, USA, 2002, http://www.pymol.org.

Reviewing Editor: David Case